Biomaterials Science

PAPER

View Article Online
View Journal | View Issue

Cite this: *Biomater. Sci.*, 2019, **7**, 3729

Improving acute cardiac transplantation rejection therapy using ultrasound-targeted FK506-loaded microbubbles in rats†

Jie Liu,‡[a,b] Yihan Chen,‡[a,b] Guohua Wang,[c] Qiaofeng Jin,[a,b] Zhenxing Sun,[a,b] Qing Lv,[a,b] Jing Wang,[a,b] Yali Yang,[a,b] Li Zhang*[a,b] and Mingxing Xie *[a,b]

Targeted delivery of immunosuppressants to allografts can increase the concentrations of drugs in pathological tissues, improve therapeutic effects and reduce unfavorable side effects. Therefore, we synthesized FK506-loaded microbubbles (FK506-MBs) for site-specific release of FK506 into transplanted hearts by the ultrasound-targeted microbubble destruction (UTMD) technique. The average particle size of FK506-MBs was 1.65 ± 0.32 μm and they had high drug loading and encapsulation efficiency. The *in vivo* drug concentration in transplanted hearts that were treated with FK506-MBs plus UTMD was about 1.64-fold higher than that in grafts that received free FK506 at the same dosage. The degree of graft rejection in the FK506-MB plus UTMD group was lower than those of other groups. Both infiltration of T cells and secretion of inflammatory cytokines were significantly reduced in the FK506-MB plus UTMD group. More importantly, the mean survival time of the grafts was significantly longer (16.00 ± 0.89 day) than those of the PBS group (6.66 ± 1.36 day) and the FK506 group (12.83 ± 1.17 day). In addition, we also found that the concentration of FK506 in whole blood was lower in the FK506-MB plus UTMD group than that in the FK506 group, which would be beneficial for reducing the side effects. Hence, our results showed that combining FK506-MBs with UTMD was an effective strategy to deliver FK506 to transplanted hearts, which can increase the local drug concentration and enhance its efficacy on rejection. Ultrasound-targeted drug release is safe and radiation-free, with great potential for clinical transformation, and could also be extended to the treatment of other graft rejection cases, such as liver transplantation, kidney transplantation and so on.

Received 24th February 2019,
Accepted 24th June 2019

DOI: 10.1039/c9bm00301k

rsc.li/biomaterials-science

1. Introduction

Heart transplantation (HT) is an effective treatment for patients with end-stage heart diseases.[1–4] The survival rate has been improved due to advances in immunosuppressive treatments. FK506, a calcineurin inhibitor, can be used to prevent and treat acute rejection (AR) after HT.[5–7]

However, FK506 exhibits poor aqueous solubility, P-gp mediated efflux, and extensive first-pass metabolism which lead to low bioavailability following oral administration.[8] In addition, traditional methods for FK506 delivery (oral or intravenous administration) can cause adverse side effects, such as nephrotoxicity, neurotoxicity, hyperlipidemia, hyperglycemia, diarrhea, hepatic dysfunction, and infection.[9,10] These side effects have been shown to be associated with the concentration of FK506 in the blood.[11,12] Therefore, improved drug delivery methods are urgently needed.

Ultrasound-targeted microbubble destruction (UTMD) has been used for drug and gene delivery.[13–15] Combined with microbubbles (MBs), drugs or genes can be delivered to specific tissues, such as tumors,[16–18] blood vessels and hearts.[19–22] When exposed to high ultrasound pressure, MBs collapse and release energy which transiently and locally enhances the permeability of the cell membrane and vessel wall of the capillary.[23,24] At the same time, drugs or genes encapsulated in MBs are released, extravasated from blood vessels and then distributed into the surrounding tissues.[25] Therefore, the dose of drugs or genes in the targeted organs or tissues is increased. Meanwhile, distribution of drugs or genes in other parts of the body is decreased and side effects are reduced.

Recently, UTMD has also been used in the treatment of some inflammatory diseases. Jun-ichi Suzuki *et al.*[26] used

[a]*Department of Ultrasound, Union Hospital, Tongji Medical College, Huazhong University of Science and Technology, Wuhan 430022, China. E-mail: zli429@hust.edu.cn, xiemx@hust.edu.cn*
[b]*Hubei Province Key Laboratory of Molecular Imaging, China*
[c]*Department of Cardiovascular Surgery, Union Hospital, Tongji Medical College, Huazhong University of Science and Technology, Wuhan 430022, China*

†Electronic supplementary information (ESI) available. See DOI: 10.1039/c9bm00301k

‡These authors contributed equally to this work.

ultrasound microbubble-mediated intercellular adhesion molecule-1 siRNAs for transfection of siRNAs into targeted arteries to inhibit the formation of arterial intima and inflammation. In addition, Wen-Shuang Sheng *et al.*[27] prepared liposomes containing the basic fibroblast growth factor (bFGF) and then combined with UTMD for delivering the bFGF to the kidney for preventing diabetic nephropathy. In this way, the concentration of the bFGF in kidneys of diabetic rats was significantly enhanced, thereby enhancing the therapeutic efficacy, and inhibiting the inflammatory response.

Considering all the above, we aimed to establish an efficient FK506 delivery strategy for treating AR after HT by combining FK506-loaded microbubbles (FK506-MBs) with UTMD. In this study, we describe the characterization of FK506-MBs and their ability to increase drug concentrations in the transplanted hearts. Then we also evaluate the feasibility and treatment efficacy of this drug delivery method in HT models. We hypothesized that compared with an intravenous injection of the same dose of FK506, this new drug delivery strategy can reduce the blood concentration of FK506, improve the drug concentration in the targeted organ, and enhance the therapeutic effects. These are the important findings that validate a novel formulation of FK506 for treating AR and present a promising strategy to reduce side effects.

2. Materials and methods

2.1 Preparation of FK506-MBs

FK506-MBs were prepared by the thin-film hydration method.[28] Briefly, 1,2-distearoyl-*sn-glycero*-3-phosphocholine (DSPC) (Avanti Polar Lipids, AL, USA) and 1,2-distearoyl-*sn-glycero*-3-phosphoethanolamine-*N*-[methoxy(polyethylene glycol)-2000] (DSPE-PEG2000) (Corden Pharma Inc, Liestal, Switzerland) at a molar ratio of 9 : 1 were dissolved in chloroform together with 250 μL FK506 stock solution (100 mg FK506 dissolved in 2.5 mL purified ethanol) (Selleck, Catalog No. S 5003). The solvent was evaporated using a steady stream of nitrogen and dried under vacuum for over 2 hours. The resulting lipid film was resuspended in a solution of 10 : 10 : 80 (v/v/v) glycerol : propylene glycol : 0.1 M Tris-buffered saline (pH 7.4) at 55 °C to a final total lipid concentration of 3 mg mL^{-1}. To prepare FK506-MBs for the experiments, the lipid solution was sub-packaged into vials (1 mL each vial). After sealing the cap, the gas in vials was replaced with perfluoropropane (C_3F_8) gas. Subsequently, the vial was mechanically shaken for 30 s using an agitator. Then, the bubble solution was stirred for 5 min at 1000 rpm, and a suspension of MBs was obtained. To separate the free drugs (not incorporated into the MBs) the FK506-MBs were washed with PBS three times by centrifugal flotation. Finally, the FK506-MBs were obtained. The blank MBs were similarly synthesized without the addition of FK506. DiI-loaded MBs (DiI-MBs) and DiR-loaded MBs (DiR-MBs) were prepared as described above using 1,1′-dioctadecyl-3,3,3′,3′-tetramethylindocarbocyanine perchlorate (DiI) (Beyotime, Haimen, China) and 1,1′-dioctadecyl-3,3,3′,3′-tetramethylindotricarbocyanine iodide (DiR) (AAT Bioquest, California, USA) instead of FK506, respectively.

2.2. Characterization of FK506-MBs

2.2.1. Particle size, drug loading efficiency, and drug encapsulation efficiency. The particle sizes of MBs pre- or post-destruction by UTMD were determined by a zeta potential analyzer (ZetaPALS, Brookhaven Instruments, USA). The concentration of MBs was determined using a hemocytometer (Qiujing, China). The morphologies of FK506-MBs and blank MBs were determined with an optical microscope (Nikon, Japan).

To evaluate the drug loading efficiency and drug encapsulation efficiency, FK506-MBs were thoroughly dissolved in methanol and sonicated for 20 min to extract the drug from MBs. FK506 was measured *via* high performance liquid chromatography (HPLC) (2695 Separation module, Waters Co., MA, USA), using a C8 column (4.6 mm × 150 mm, 5 μm) at 50 °C. The mobile phase solution consisted of 70 : 30 (v : v) mixtures of acetonitrile and 0.1% phosphoric acid solution in water. The flow rate was set at 1 mL min^{-1} and FK506 was monitored at 210 nm. The drug encapsulation efficiency and drug loading efficiency were calculated using the following formulas:

$$\text{Drug encapsulation efficiency}\,(\%) = \text{weight of FK506 in MBs}/\text{weight of the total amount of FK506 in preparation of MBs} \times 100\%$$

$$\text{Drug loading efficiency}\,(\%) = \text{weight of FK506 in MBs}/\text{weight of total FK506} - \text{MBs} \times 100\%$$

2.2.2. FK506-MB stability *in vitro*. The variations of the storage time and temperature may result in changes of drug loading efficiency and encapsulation efficiency. We monitored the leakage of FK506 from FK506-MBs under different conditions. FK506-MBs were stored in small glass vials at 4 °C or 37 °C for 1 h, 3 h, 5 h, 12 h and 24 h, respectively, and periodically centrifuged. The collected solution was used to estimate the amount of FK506 leakage by HPLC. The FK506 leakage percentage (%) = weight of the leakage of FK506/weight of FK506 in MBs × 100%.

2.2.3 *In vitro* UTMD-triggered FK506 release. An ultrasound probe (Sonitron 2000 V, Japan) was used to trigger the release of FK506 from FK506-MBs. Briefly, 1 mL ($4.35 \pm 0.18 \times 10^9$ MBs mL^{-1}) FK506-MBs were diluted to 10 mL. Then 100 μL diluted FK506-MBs were mixed with 400 μL PBS and injected into an agarose mold with a 5 mm diameter chamber. Subsequently, these FK506-MBs were destructed by UTMD (ultrasound frequency = 1 MHz; duty cycle = 50%; and ultrasound intensity = 2 w cm^{-2}) with various irradiation times (1 min, 2 min, and 3 min). Finally, the sonicated samples were collected and centrifuged for 5 min at 1000 rpm. Then the underlying liquid was analyzed by HPLC to quantify the amount of FK506 released from FK506-MBs.

2.3. *In vivo* studies

2.3.1. Heterotopic HT models. Male Brown Norway (BN, 180–230 g) and Lewis (180–230 g) rats were provided by Vital River Laboratory (Beijing, China). All animal procedures were performed in accordance with the Guidelines for Care and Use of Laboratory Animals of the National Institutes of Health (NIH), and approved by the Institutional Animal Care and Use Committee (IACUC) of Tongji Medical College, Huazhong University of Science and Technology. Heterotopic HT was performed according to the method previously reported by us.[29] In the allograft group the donor heart was transplanted from a BN rat to a Lewis rat, while in the isograft group the graft was transplanted from a Lewis rat to another Lewis rat. Briefly, after the donor was anesthetized, its heart was harvested in less than 40 minutes and placed in 4 °C saline until transplantation. The transplantation was performed with end-to-side anastomoses of the donor ascending aorta to the recipient abdominal aorta and the donor pulmonary artery to the vena cava of the recipient rat, respectively. After operation, the rats were allowed to recover in a warmed cage and housed in a sterile environment.

2.3.2. Optical imaging *ex vivo*. DiR-MBs were used as substitutes for FK506-MBs to investigate whether FK506-MBs + UTMD could enhance the concentration of the drug at myocardial tissues. Allograft group rats were divided into three groups randomly: (1) PBS group; (2) DiR (dissolved in purified ethanol) alone; and (3) DiR-MBs + UTMD (similar absorption intensity to DiR). The ultrasound probe was placed at transplanted hearts for triggering drug release as shown in Fig. 1. The optimized UTMD parameters (ultrasound frequency = 1 MHz; duty cycle = 50%; ultrasound intensity = 2 w cm^{-2}; and irradiation time = 2 min) were maintained throughout the following experiments. At 10 min, 30 min, 60 min, 180 min and 360 min after the treatment, all rats were euthanized, and major organs including hearts, livers, cardiac grafts, spleens, lungs and kidneys were harvested. Then *ex vivo* images of the organs were captured and quantified using a small animal imaging system (*In vivo* FX PRO, BRUKER).

2.3.3. Confocal laser scanning microscopy (CLSM). Further experiments were performed to determine whether FK506-MBs can pass through the endothelial barrier and capillary walls and locate in the myocardial tissues. DiI-MBs were used instead of FK506-MBs. Allograft group rats were divided into two groups randomly: (1) DiI (dissolved in purified ethanol) alone; and (2) DiI-MBs + UTMD (similar absorption intensity to DiI). The UTMD parameters used were the same as those in the above experiment. After 30 min, the rats were euthanized and infused with 300 mL PBS to clear the blood from circulation. The extracted hearts were embedded in the O.C.T. compound (Sakura Finetek Japan Co., Ltd, Tokyo) and cut into 7 μm-thick sections. DAPI was used for staining cell nuclei and an anti-CD31 antibody (ab64543, Abcam, Cambridge, UK) was used to identify myocardial vessels. Finally, the images were obtained with CLSM.

2.3.4. Quantification of the concentration of FK506 in transplanted heart tissues and whole blood. The allograft group was then further divided into 2 subgroups: (1) FK506 group and (2) FK506-MB + UTMD group. The FK506 group and FK506-MB + UTMD group were treated with the same dose of FK506 (1 mg per kg body weight). To quantify the concentration of FK506 in transplanted heart tissues, 12 rats (six in each group) were sacrificed 30 min after the experiment, after which the transplanted hearts were harvested and immediately stored at −80 °C. Another 12 rats (six in each group) were randomly divided into the FK506 group and the

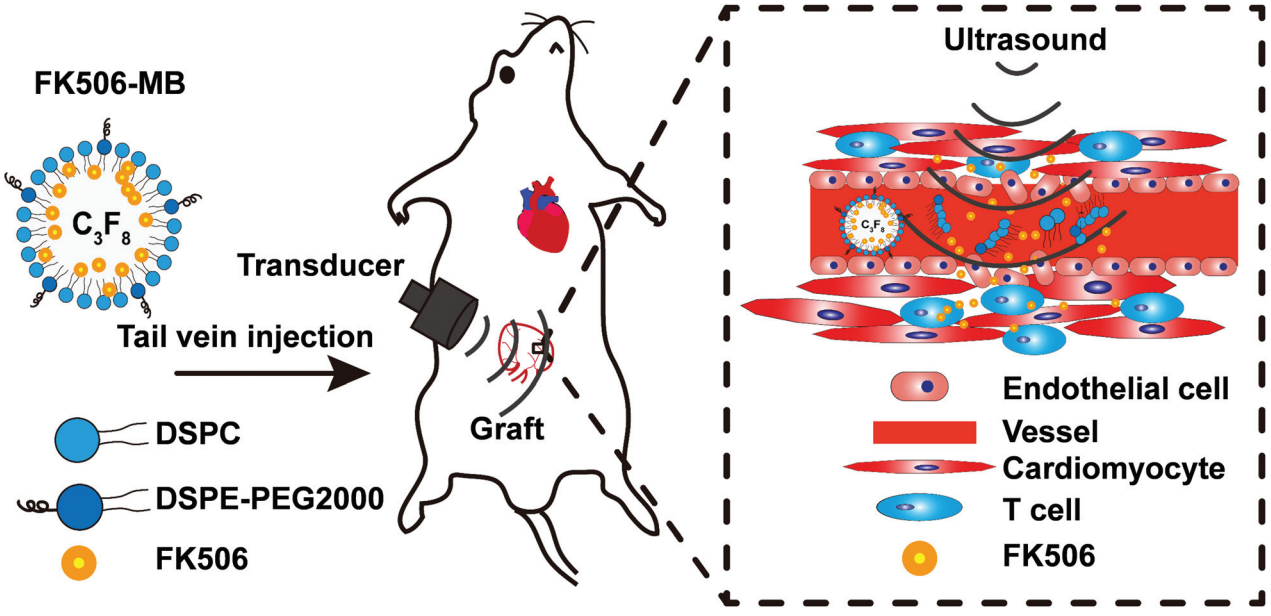

Fig. 1 Schematic diagram of the therapeutic process of FK506-MBs + UTMD *in vivo*.

FK506-MB + UTMD group to compare the concentrations of FK506 in whole blood at 2 h and 4 h after treatment. The amount of FK506 was measured by ultra-high performance liquid chromatography tandem mass spectrometry (UPLC–MS). Analysis was performed using an UltiMate 3000 RS system (Thermo Fisher Scientific Inc., USA) coupled with a TSQ Quantum (Thermo Fisher Scientific Inc., USA). Chromatographic separation was achieved using a Hypersil GOLD chromatography column (100 × 2.1 mm, 1.9 μm). Mass spectrometry (MS) was performed with electrospray ionization (ESI) in positive ion mode. Mass spectrometric analyses were performed in selective reaction detection (SRM) mode.

2.3.5. Western blotting. Western blotting was used to detect the expression of CD3 and secretion of IL-2 and IFN-γ in transplanted hearts. Briefly, proteins extracted from transplanted heart tissues were separated on 15% SDS-PAGE and transferred to polyvinylidene difluoride (PVDF) membranes. The PVDF membranes were blocked with 5% skimmed milk for 2 h. Then, they were incubated with the primary antibodies against CD3 (ab5690, abcam), IL-2 (ZI091710A, R&D), IFN-γ (sc-59992, SANTA CRUZ), or GAPDH (ab9485, abcam) overnight at 4 °C, followed by incubation with an HRP-conjugated secondary antibody for 2 h at room temperature. The specific bands were detected using Super ECL reagent. Images were obtained by using a BioSpectrum 600 Imaging System (UVP, CA, USA). The intensity of the GAPDH band was used as a loading control for comparison between samples.

2.3.6. Histological analysis and graft survival. To evaluate the therapeutic efficacy, recipients were treated once a day for continuous five days since the day of surgery. The animals were euthanized at day 6 post-HT. Transplanted hearts were perfused with PBS, removed and embedded in paraffin. Then the tissues at the level of the papillary muscles were sliced and stained with haematoxylin and eosin. AR was evaluated according to the 2004 working formulation of the International Society for Heart and Lung Transplantation (ISHLT).[30] The infiltration of T cells and secretion of proinflammatory cytokines were evaluated by immunofluorescence staining. Specific antibodies used included anti-CD3 antibody (ab5690, Abcam, Cambridge, UK), anti-interferon gamma (ab216642, Abcam, Cambridge, UK), and anti-IL-2 antibody (ZI091710A, R&D). In the graft survival studies, another 24 rats were used to evaluate the mean survival time (MST). The grafts were monitored by daily abdominal palpation, and the endpoint of the grafts was defined as the cessation of palpable heart beating.

2.4. Statistics

Results were presented as the means ± standard error of the mean (SEM) of at least three independent measurements. Statistical comparison of the survival time was determined by a Log-rank (Mantel–Cox) test, and other statistical evaluations were carried out with unpaired two-tailed student's *t*-tests. A *P* value less than 0.05 ($P < 0.05$) was considered as statistically significant.

3. Results

3.1. Characterization of FK506-MBs and drug release under UTMD *in vitro*

FK506 encapsulated in MBs was detected by HPLC. The drug encapsulation efficiency increased with the initial dose from 0 to 2.0 mg, after which it decreased (Fig. 2A). Therefore, we used the initial dose of 2.0 mg to prepare FK506-MBs. The average drug payload was 1.51 ± 0.18 mg mL^{-1}, the drug encapsulation efficiency was 77.6 ± 8.0%, and the drug loading efficiency was 33.41 ± 2.69%.

The mean diameter, concentration, and PDI of the blank MBs and FK506-MBs under optimized conditions are summarized in Table 1. Fig. 2B shows the bright field of the blank MBs and FK506-MBs. The microscopy images revealed that all blank MBs and FK506-MBs were spherical and dispersive. Fig. 2C shows the diameter distribution of the blank MBs and FK506-MBs. The weight of the drug in FK506-MBs was relatively stable at 4 °C for 5 h. Drug leakage was only 6.0 ± 1.0% after 24 h when FK506-MBs were stored at 4 °C, but the leakage changed from 2.10 ± 0.3% at 1 h to 4.30 ± 0.2% at 5 h and 15.67 ± 2.0% after 24 h of storage at 37 °C (Fig. 2D).

The release of FK506 from FK506-MBs could be controlled by UTMD, and the irradiation time was an important parameter. The drug releasing efficiency was 49.51 ± 5.0% at 1 min and increased to 72.55 ± 2.0% at 2 min. Nevertheless, the release of FK506 only improved slightly with the increase of the irradiation time, reaching 76.52 ± 3.0% at 3 min (Fig. 2E).

The time–intensity curve (TIC) from ultrasound images demonstrated that FK506-MBs and blank MBs had similar life time *in vivo* (Fig. S1†). Therefore, after drug loading, FK506-MBs appeared to retain good acoustic and physical properties similar to pure blank MBs.

3.2. Drug-loaded MBs plus the UTMD technique improve the concentration of drugs in transplanted heart tissues

After 10 min, 30 min, 60 min, 180 min and 360 min of treatment, the fluorescence intensities of the cardiac graft in the DiR-MB + UTMD group were significantly stronger than those in the pure DiR group (Fig. 3A and B). In the DiR-MB + UTMD group, the fluorescence intensity of the cardiac graft at 30 min was stronger than that at 10 min ($p < 0.05$). The fluorescence intensity at 60 min was not significantly different from that at 30 min. Then the fluorescence intensity decreased at 180 min, and further decreased at 360 min. In addition, we found that most of the organs showed the fluorescence of DiR after administration, while the fluorescence intensities of the liver, spleen and lung were stronger than those of other organs.

Fig. 3C shows the deposition of DiI in transplanted heart tissues in the DiI group and DiI-MB + UTMD group. When irradiated with ultrasound, DiI-MBs were destroyed and released DiI to the myocardial interstitium in transplanted hearts. CD31 was used to mark blood vessels and DAPI was applied to dye nuclei. As shown in Fig. 3C, red fluorescence was detected in the graft section in the DiI-MB + UTMD group. But, the red

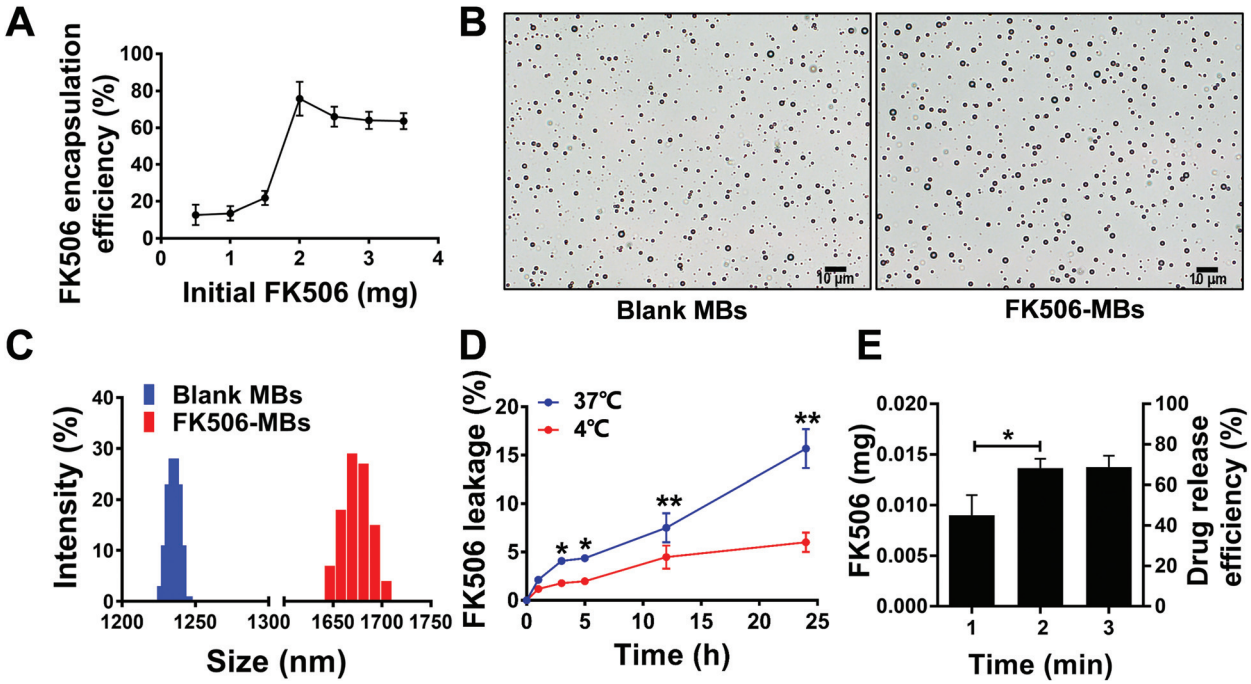

Fig. 2 Characterization of FK506-MBs and *in vitro* UTMD-triggered drug release. (A) Quantification of FK506 encapsulated in FK506-MBs. (B) Microscopy bright field images of blank MBs and FK506-MBs. (C) Size distribution of blank MBs and FK506-MBs. (D) Cumulative release of FK506 from FK506-MBs into PBS at 4 °C and 37 °C at different time points. (E) The effect of the UTMD irradiation time on drug release from FK506-MBs *in vitro* (n = 6), *P < 0.05; **P < 0.01.

Table 1 Characteristics of FK506-MBs and blank MBs

	Mean diameter (μm)	Concentration (10^9 mL^{-1})	PDI
FK506-MBs	1.65 ± 0.32	4.35 ± 0.18	0.16 ± 0.09
Blank MBs	1.20 ± 0.21	5.71 ± 0.15	0.12 ± 0.07

fluorescence was not discovered in the myocardial interstitium in the DiI group.

We further examined the concentration of FK506 in transplanted heart tissues by UPLC-MS. As shown in Fig. 3D, FK506 was detected in the transplanted heart tissues in the FK506 group and FK506-MB + UTMD group. More importantly, the concentration of FK506 was significantly greater in the FK506-MB + UTMD group (3.17 ± 0.38 μg g^{-1} of tissue) than that in the FK506 group (1.93 ± 0.29 μg g^{-1} of tissue). We also analysed the concentration of FK506 in the whole blood. The FK506 levels in whole blood at 2 h and 4 h were significantly lower in the FK506-MB + UTMD group than that in the FK506 group (Fig. S2†). These results showed that FK506-MBs combined with UTMD for drug delivery increased the drug concentration in the transplanted heart tissues and decreased the concentration in the whole blood.

3.3. FK506-MBs combined with UTMD treatment attenuated the degree of AR

HE staining was used to analyze the pathological changes after treatments. Fig. 4 shows the degree of AR in different groups. In the isograft group, all rats had normal myocardial tissues and no inflammatory infiltration, and they were classified as grade 0 R according to ISHLT standardized cardiac biopsy grading. All grafts in the PBS group were graded as grade 3 R rejection which was characterized with diffuse inflammatory cell infiltration, large areas of coagulative myocardial cell necrosis, hemorrhages, edema and obviously vasculitis (Fig. 4A). In contrast, in the FK506 group 50% grafts showed weaker rejection, and these graft rejections were fit into the 1 R or 2 R grade of rejection. The rejection 1 R indicates only one focus of myocardial cell damage. However, 2 R represents more than two focuses of inflammatory cell infiltration and myocardial cell damage. Compared with the FK506 group, about 83% grafts in the FK506-MB + UTMD group belonged to the 1 R or 2 R grade of rejection (Fig. 4B).

3.4. FK506-MBs combined with UTMD treatment reduced T cell infiltration and the expression of inflammatory cytokines in transplanted heart tissues

FK506 is mainly used to modulate cell-mediated immune responses, especially for inhibiting the proliferation of T cells and the secretion of inflammatory cytokines. As shown in Fig. 5, a high level of CD3$^+$ cell infiltration was observed in the PBS group. Comparatively, the FK506 group and FK506-MB + UTMD group showed a markedly reduced CD3$^+$ lymphocyte infiltration. More importantly, there was dramatically diminished infiltration of CD3$^+$ cells in the FK506-MB + UTMD group *versus* the FK506 group.

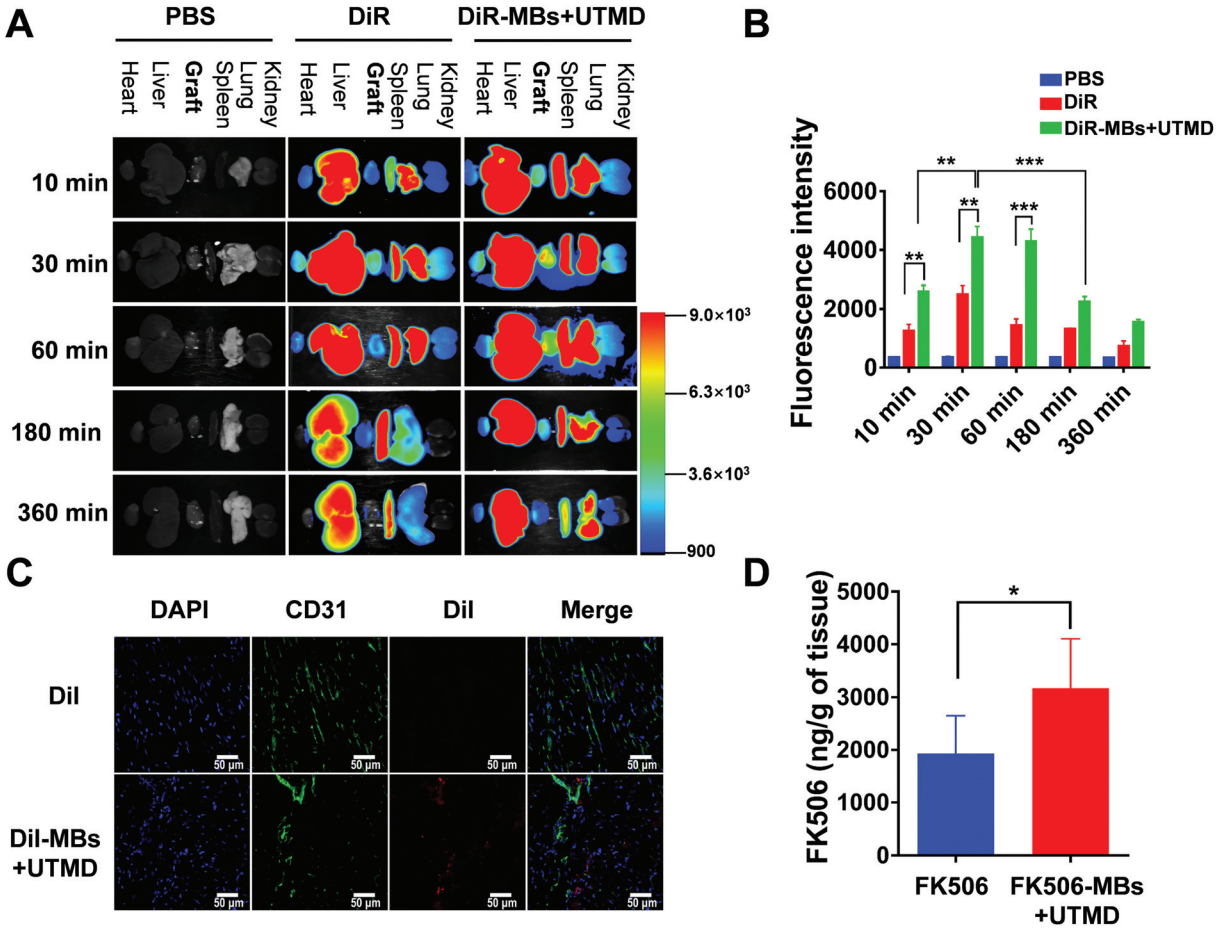

Fig. 3 Drug-loaded MB plus UTMD technique improves the concentration of drugs in transplanted heart tissues. (A) *Ex vivo* images of the major organs 10 min, 30 min, 60 min, 180 min and 360 min after injection of DiR and DiR-MBs, respectively. (B) Quantitative analysis of the fluorescence intensity in the cardiac graft at 10 min, 30 min, 60 min, 180 min and 360 min (n = 3). (C) CLSM images show that DiI deposition in transplanted heart tissues increases in the DiI-MB + UTMD group. (D) *In vivo* quantification of the FK506 concentration by UPLC-MS in transplanted hearts 30 min after treatment (n = 6), *P < 0.05, **P < 0.01, ***P < 0.001.

Then, the expression levels of IFN-γ and IL-2 in transplanted heart tissues were evaluated by immunofluorescence staining and western blot. We observed elevated IFN-γ (Fig. 6) and IL-2 (Fig. 7) expression in the PBS group, while the expression of these factors decreased in the FK506 group. Moreover, IFN-γ and IL-2 expression levels were significantly less in the FK506-MBs + UTMD group compared to those of other groups. Therefore, our study proved that FK506-MBs combined with UTMD treatment reduced T cell infiltration and the secretion of inflammatory cytokines in transplanted heart tissues.

3.5. FK506-MBs combined with UTMD treatment prolonged the survival of the transplanted hearts

To evaluate the therapeutic efficacy, the survival time of the transplanted hearts was observed in all groups. The survival data are graphically depicted in Fig. 8. All animals in the isograft group had good pulsation during the observation period and survived for more than 30 days. However, allografts were promptly rejected in the PBS group and the MST of the cardiac allografts was 6.66 ± 1.36 days. But the MST was significantly prolonged in the FK506 group (12.83 ± 1.17 days *vs.* PBS group, P < 0.0001) and FK506-MB + UTMD group (16.00 ± 0.89 days *vs.* PBS group, P < 0.0001). The results also illustrated that the treatment with FK506-MBs combined with UTMD significantly prolonged the cardiac allograft survival time than that with FK506 alone (P < 0.0001).

4. Discussion

Cardiac AR is essentially a cell-mediated immune reaction. T cells play a key role in the pathogenesis and development of AR. Activated T cells release cytokines to cause immunologic injuries or damage the adjacent tissues directly. Inhibition of T cell proliferation and activation is an effective method to treat AR.[31]

FK506, also known as tacrolimus, is an immunosuppressive drug used for AR treatment clinically. It inhibits the production of IL-2, a molecule that promotes the development

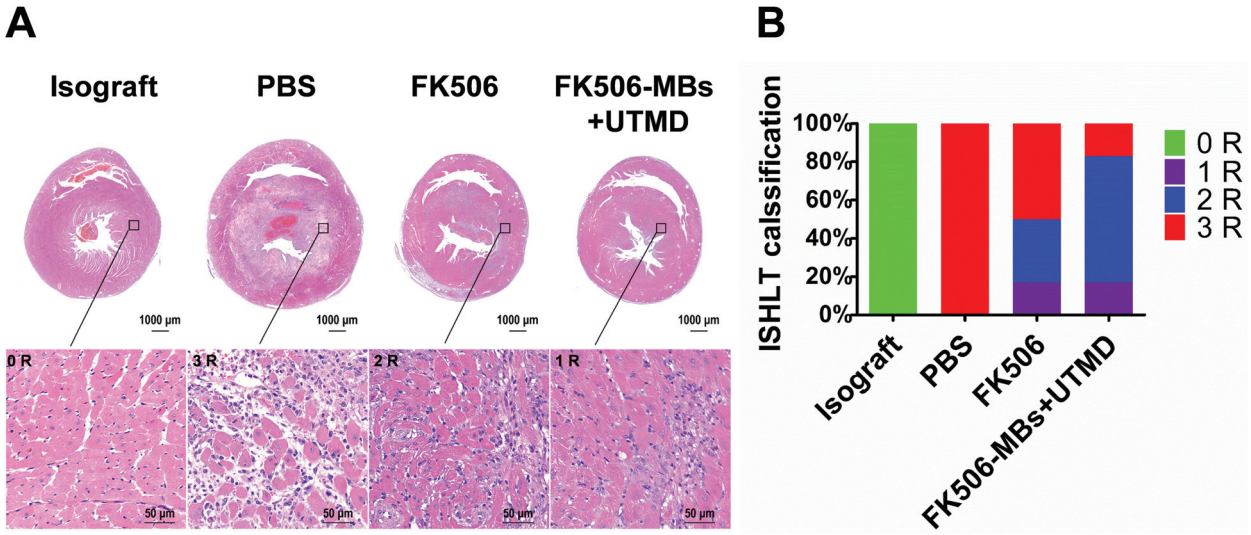

Fig. 4 Histological analysis on the 6th day after treatment. (A) HE staining was used to evaluate the degree of AR. 0R: in the isograft group there is no evidence of inflammation or myocyte damage; 3R: a high power view in the PBS group showed widespread inflammatory cell infiltration and some damage; 2R: a high power view in the FK506 group showed focal inflammatory infiltration, myocyte damage and architectural distortion; 1R: a high power view in the FK506-MB + UTMD group showed one focus of inflammatory cell infiltration without myocyte damage. (B) AR grades of the isograft, PBS, FK506, and FK506-MB + UTMD groups (n = 6).

and proliferation of T cells, and thereby suppresses the rejection response. However, when given by intravenous or oral administration, the risk of adverse reactions is unavoidable.[6] Localized delivery of immunosuppressive agents is an alternative to safeguard the transplanted hearts while minimizing the side effects of systemic immunosuppression.

MBs, which consist of fluorocarbon gas encapsulated by a lipid or a protein shell, are not only an ideal contrast agent for ultrasound imaging, but also an excellent drug carrier for therapy.[32] Drug-loaded MBs could be manufactured by electrostatic or hydrophobic interactions, or physical encapsulation. Due to its good lipid solubility, FK506 can be loaded onto the membrane of microbubbles.[33] In the current study, the drug loading efficiency of FK506-MBs was up to 33.41 ± 2.69%, which was much higher than that of FK506-loaded poly(ethylene glycol)-poly(D,L-lactide) nanoparticles (FK506/MPEG-PLA). Although the drug loading ratio (%) varied with the ratio of FK506 to MPEG-PLA, the maximum drug loading ratio was still less than 20%.[34] In order to change the poor aqueous solubility of FK506, Saba Khan *et al.* designed a stable nanostructured lipid carrier for FK506 delivery. Different methods of preparation had been tried, but the drug loading efficiency was still under 10%.[35] Moreover, to prolong the controlled release and increase the bioavailability of FK506, nano-scale liposomes with a binary lipid constituent have gained a lot of attention.[36] Yikang Dai *et al.* had shown that the drug encapsulation efficiency of liposomes was more than 90%, significantly higher than that of the FK506-MBs which we prepared (about 77.6 ± 8.0%). However, the drug loading efficiency of liposomes is lower than that of FK506-MBs.[37] The reason for this might be the bigger size of MBs relative to that of nanoparticles. For a single particle, the larger the particle size, the larger the surface area and the more drugs it contains. Similar phenomena have also been confirmed in Ryo Kojima's study.[38] He prepared FK506-loaded microspheres composed of poly (lactic-*co*-glycolic acid) (PLGA) and/or polylactic acid (PLA). The drug loading ratio of FK506-loaded microspheres was about 30%, which was close to the level found in our FK506-MBs.

UTMD has been shown to be capable of improving the efficiency of microbubble-based drug delivery across biological barriers without causing cellular damage.[21] By focusing the ultrasound beam on transplanted hearts, the ultrasound only triggers cavitation of MBs (oscillation and collapse) at the heart site to locally enhance the permeability of the endothelial barrier and cell membrane. Then, the drug extravasation can be improved.[39,40] The concentration of FK506 in transplanted hearts of the FK506-MBs + UTMD group was 1.64-fold greater than that of the FK506 group after 30 min administration, which was similar to the result of the *ex vivo* optical imaging. The fluorescence intensity of DiR was 1.7-fold higher in the DiR-MB + UTMD group compared to that in the DiR group at 30 min. After destruction, MBs split into nano-sized fragments (Fig. S3†), which may delay the degradation and metabolism of drugs. We found that the fluorescence intensity was not significantly decreased at 60 min after UTMD treatment, while it obviously decreased in the pure DiR group.

After 5 days of continuous treatment, the infiltration of T cells in the myocardium was significantly reduced, as well as IL-2 and IFN-γ secretion. The T lymphocyte is a major factor in myocardial injury during acute rejection.[41] Hence inhibition of T cell infiltration can significantly reduce the degree of myocardial injury. At the same time, reduction of T cells leads to decreased secretion of inflammatory factors, such as IL-2 and IFN-γ. IL-2 is an interleukin, mainly secreted by activated $CD4^+$

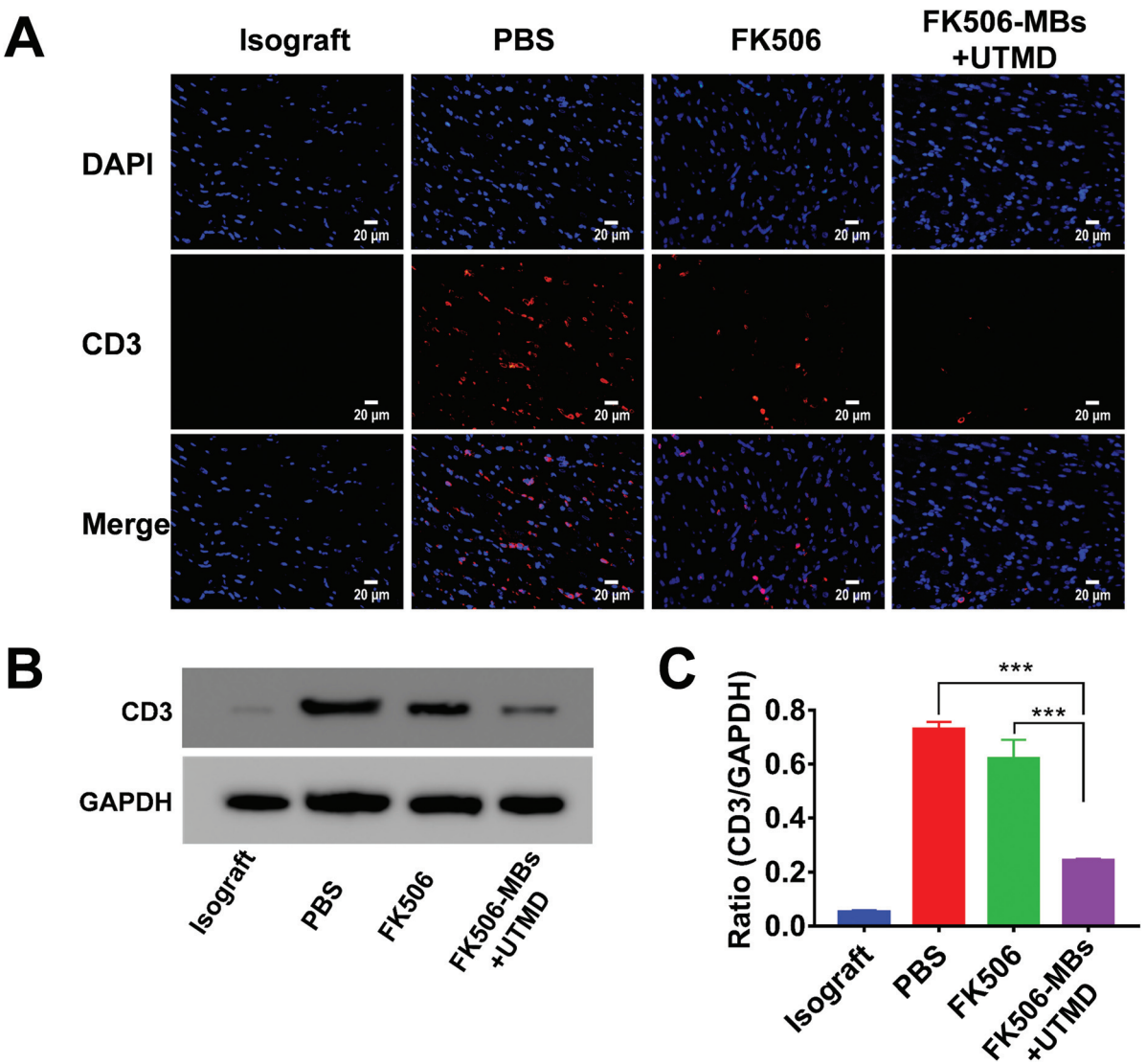

Fig. 5 The expression of $CD3^+$ T cells in transplanted hearts. (A) Immunofluorescence staining showed that in the FK506-MB + UTMD group, the $CD3^+$ cells in the myocardial tissue were significantly reduced (n = 6); (B) representative blots of the expression of CD3 in transplanted heart tissues in different groups. (C) Relative quantitative analysis of the CD3 protein in each group (n = 3), ***P < 0.001.

T cells and $CD8^+$ T cells. Its main function is to stimulate T cell proliferation and promote the differentiation of T cells into effector T cells and memory T cells.[42,43] The reduction of IL-2 also reduces T cell infiltration in grafts. IFN-γ is mainly secreted by T helper cells and cytotoxic T cells. As a pro-inflammatory factor, it can enhance T-cell-mediated cellular immunity and aggravate the AR after organ transplantation.[44] Reducing the secretion of IFN-γ can effectively reduce the damage of T cells to myocardium. Therefore, the attenuation of these inflammatory factors is beneficial for prolonging the survival of the transplanted hearts. On the other hand, the drug concentrations in transplanted hearts were increased by UTMD, but it only accounted for a small fraction of the initial injection dose. Most of the drugs were distributed systematically and could reach organs of the immune system, such as the spleen. As the biggest peripheral immune organ, the spleen plays an important role in the immune reaction, including activation and proliferation of T cells. Therefore, this part of drugs could reduce T cell infiltration in transplanted hearts by inhibiting T cell activation and proliferation. As a result of the above two reasons, the therapeutic efficacy was remarkably enhanced by FK506-MBs combined with UTMD. What's more, the concentration of FK056 in whole blood was lower in the FK506-MB + UTMD group than that in the FK506 group, which may be beneficial for reducing the side effects.

In addition, UTMD mediated drug delivery is safe and non-invasive, with great potential for clinical transformation. At present, UTMD targeted drug delivery has achieved good results in the treatment of neoplastic diseases and Alzheimer's disease. UTMD open blood–brain barrier treatment of Alzheimer's disease has been applied in clinical practice.[45] What's more, many studies have used UTMD for heart dis-

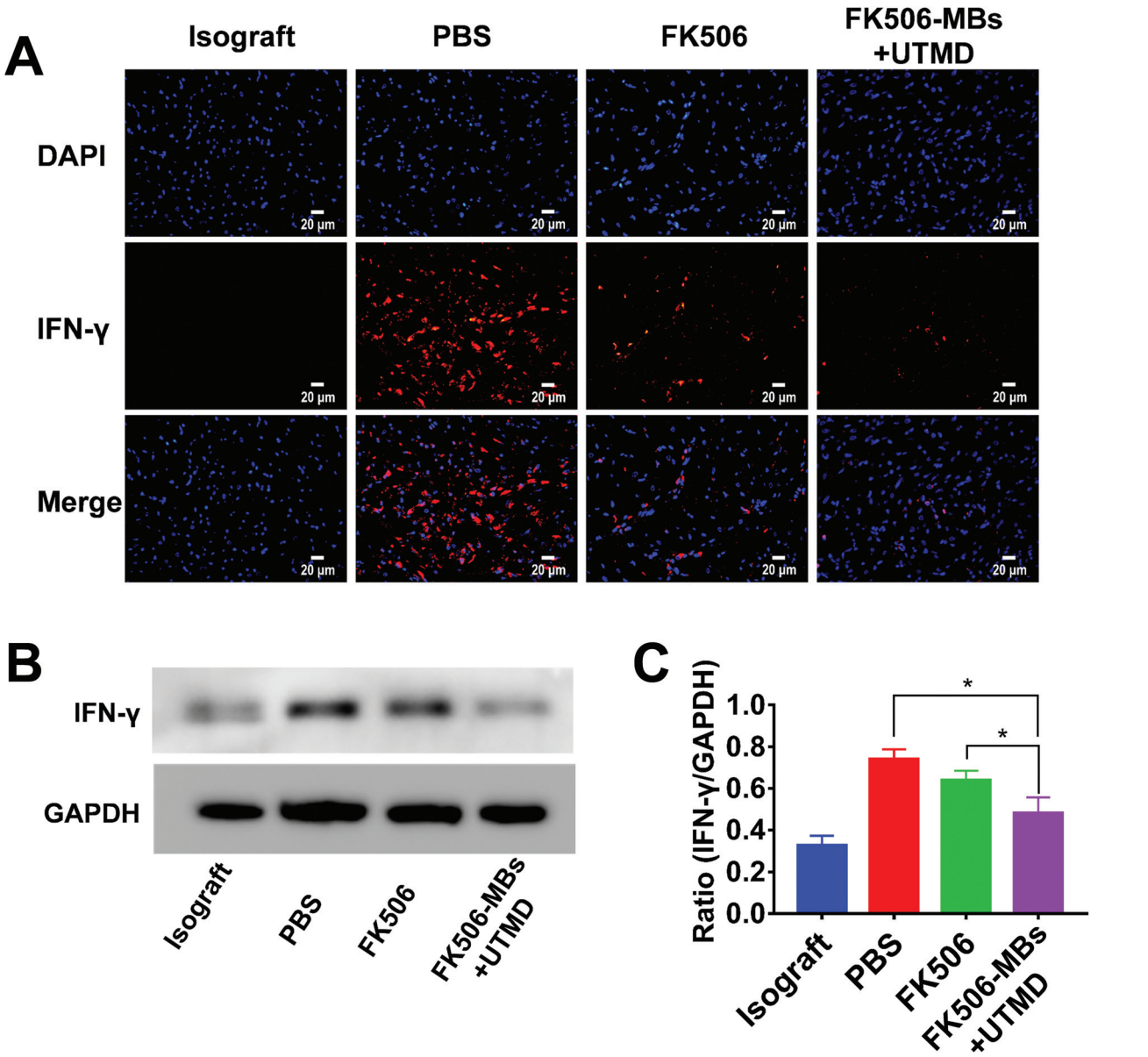

Fig. 6 The secretion of IFN-γ was analysed by immunofluorescence staining and western blot. (A) After treatment with FK506, the secretion of IFN-γ was decreased, and this effect was more pronounced in the FK506-MB + UTMD group (n = 6); (B) representative blots of the expression of IFN-γ in transplanted heart tissues in different groups. (C) Relative quantitative analysis of the IFN-γ protein in each group (n = 3) *P < 0.05.

eases. These results indicated that UTMD did not cause heart injury.[46] In our study, we also found that MBs and UTMD did not affect blood cells (Table S1†). They also did not produce toxicity (Fig. S4†) and did not cause pathological damage to the heart and other vital organs (Fig. S5†). Therefore, UTMD is a promising method for drug delivery.

Although the results obtained in this study were encouraging, there are some limitations concerning the research. First, the sample used in our experiment was small. Second, there are some practical issues which need to be addressed in the clinical application of the UTMD technique for drug delivery. Even though several studies have reported that UTMD is a safe technique for the diagnosis and treatment of diseases,[47,48] the long-term impact of continuous and repeated use of UTMD still requires further exploration.

It has to be pointed out that we used an abdominal heterotopic heart transplantation model in this study. The heterotopic heart transplantation model in rats and mice is the most commonly used model to study the allograft immune response.[29,49,50] The transplantation was performed with anastomoses of the donor ascending aorta and pulmonary artery to the abdominal aorta and vena cava of recipient rats. Because the rat strains were different, the major histocompatibility antigens between donors and recipients were mismatched. The recipient immune system recognized alloantigen. T cells were activated and migrated to graft hearts to

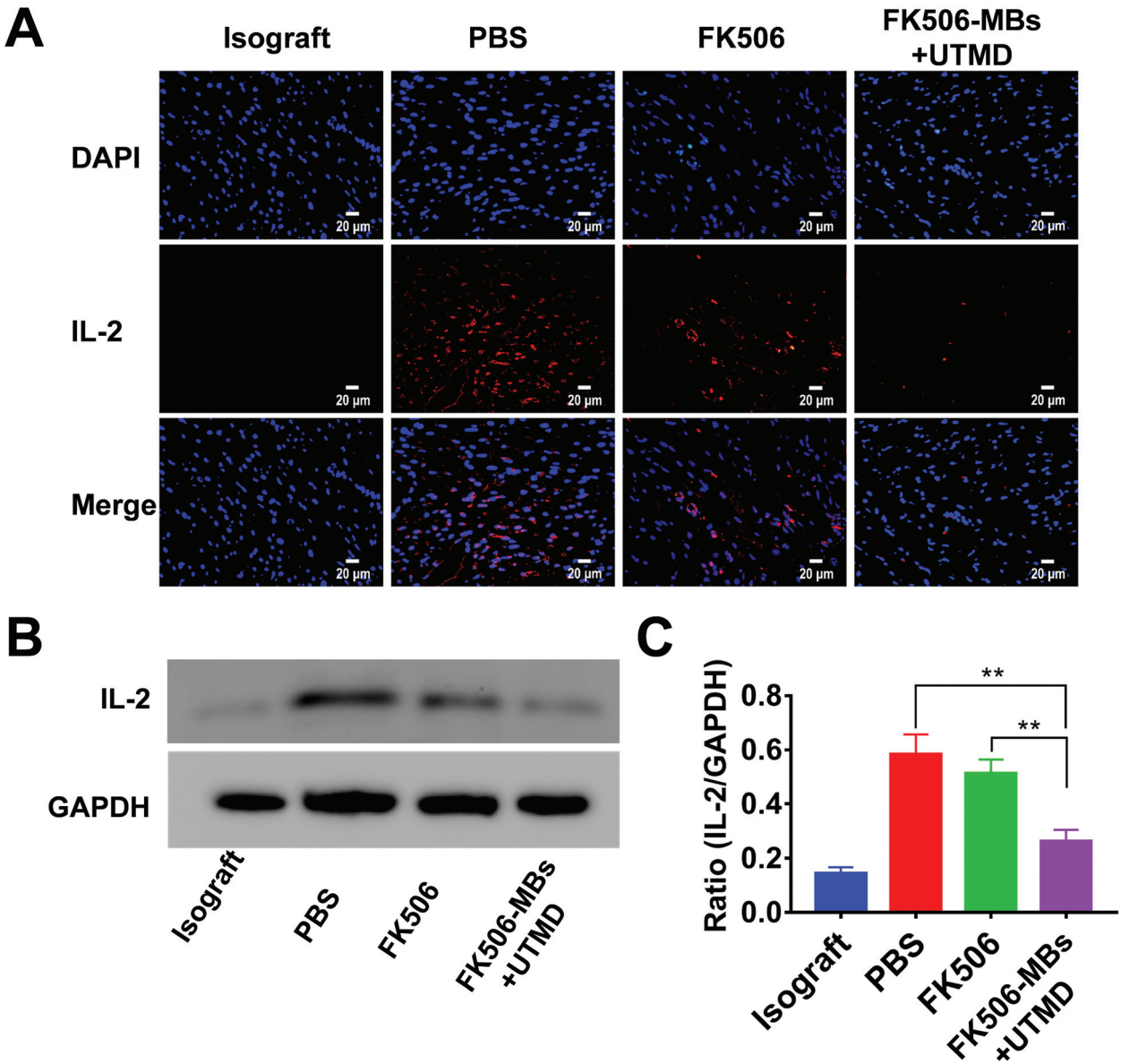

Fig. 7 The secretion of IL-2 was analysed by immunofluorescence staining and western blot. (A) After treatment with FK506, the secretion of IL-2 was decreased, and this effect was more pronounced in the FK506-MB + UTMD group (n = 6); (B) representative blots of the expression of IL-2 in transplanted heart tissues in different groups. (C) Relative quantitative analysis of the IL-2 protein in each group (n = 3), $^{**}P < 0.01$.

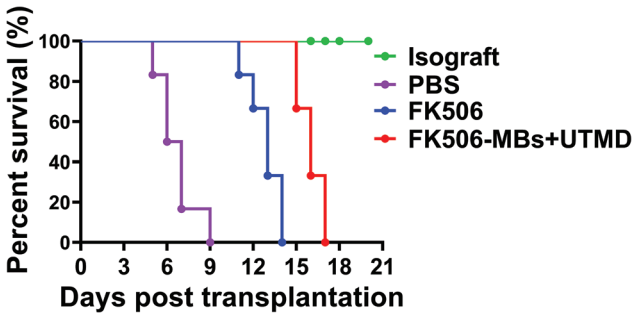

Fig. 8 The survival time of the cardiac grafts. In the FK506-MB + UTMD group, the mean survival time of the grafts was significantly longer (16.00 ± 0.89 day) than those of the PBS group (6.66 ± 1.36 day) and the FK506 group (12.83 ± 1.17 day) (n = 6).

induce rejection, which was similar to the pathological process of rejection in orthotopic heart transplantation.

5. Conclusion

In conclusion, lipid microbubbles are excellent drug carriers for FK506. FK506-MBs had a high drug loading efficiency. Combined with UTMD, FK506 could be selectively delivered to transplanted heart tissues and released locally, which enhanced the local drug concentration while reducing systemic cytotoxic effects. In addition, with the help of ultrasonic cavitation, the therapeutic effect of drugs was further strengthened. These data may lead to future clinical translation to

combat AR in cardiac transplant patients. Furthermore, this strategy potentially can be extended to transplant rejection in other organs, such as the liver and kidney.

Conflicts of interest

There are no conflicts to declare.

Acknowledgements

This work was supported by the National Natural Science Foundation of China [grant numbers 81530056, 81727805, 81471678, 81271582, 81671705, 81771851, and 81701716] and HUST Interdisciplinary Innovation Team [0118530300].

Notes and references

1 F. M. Hoffman, *J. Cardiovasc. Nurs.*, 2005, **20**, S31–S42.
2 J. K. Patel, M. Kittleson and J. A. Kobashigawa, *Surgeon*, 2011, **9**, 160–167.
3 Y. Chen, L. Zhang, J. Liu, P. Zhang, X. Chen and M. Xie, *Transplantation*, 2017, **101**, 1977–1986.
4 S. A. Hunt, *N. Engl. J. Med.*, 2006, **355**, 231–235.
5 J. A. Kobashigawa and J. K. Patel, *Nat. Clin. Pract. Cardiovasc. Med.*, 2006, **3**, 203–212.
6 J. Lindenfeld, G. G. Miller, S. F. Shakar, R. Zolty, B. D. Lowes, E. E. Wolfel, L. Mestroni, R. L. Page 2nd and J. Kobashigawa, *Circulation*, 2004, **110**, 3858–3865.
7 S. A. Hunt and F. Haddad, *J. Am. Coll. Cardiol.*, 2008, **52**, 587–598.
8 V. Nekkanti, J. Rueda, Z. Wang and G. V. Betageri, *AAPS PharmSciTech*, 2016, **17**, 1019–1029.
9 D. H. Peters, A. Fitton, G. L. Plosker and D. Faulds, *Drugs*, 1993, **46**, 746–794.
10 L. J. Scott, K. McKeage, S. J. Keam and G. L. Plosker, *Drugs*, 2003, **63**, 1247–1297.
11 Y. Bottiger, C. Brattstrom, G. Tyden, J. Sawe and C. G. Groth, *Br. J. Clin. Pharmacol.*, 1999, **48**, 445–448.
12 T. Yoshida, K. Nakanishi, T. Yoshioka, Y. Tsutsui, A. Maeda, H. Kondo and K. Sako, *Eur. J. Pharm. Biopharm.*, 2016, **100**, 58–65.
13 T. Boissenot, A. Bordat, E. Fattal and N. Tsapis, *J. Controlled Release*, 2016, **241**, 144–163.
14 S. R. Sirsi and M. A. Borden, *Theranostics*, 2012, **2**, 1208–1222.
15 R. Zhao, X. Liang, B. Zhao, M. Chen, R. Liu, S. Sun, X. Yue and S. Wang, *Biomaterials*, 2018, **173**, 58–70.
16 C. H. Fan, C. Y. Ting, H. L. Liu, C. Y. Huang, H. Y. Hsieh, T. C. Yen, K. C. Wei and C. K. Yeh, *Biomaterials*, 2013, **34**, 2142–2155.
17 H. Nesbitt, Y. Sheng, S. Kamila, K. Logan, K. Thomas, B. Callan, M. A. Taylor, M. Love, D. O'Rourke, P. Kelly, E. Beguin, E. Stride, A. P. McHale and J. F. Callan, *J. Controlled Release*, 2018, **279**, 8–16.
18 S. M. Chowdhury, T. Y. Wang, S. Bachawal, R. Devulapally, J. W. Choe, L. Abou Elkacem, B. K. Yakub, D. S. Wang, L. Tian, R. Paulmurugan and J. K. Willmann, *J. Controlled Release*, 2016, **238**, 272–280.
19 Y. Z. Zhao, X. Q. Tian, M. Zhang, L. Cai, A. Ru, X. T. Shen, X. Jiang, R. R. Jin, L. Zheng, K. Hawkins, S. Charkrabarti, X. K. Li, Q. Lin, W. Z. Yu, S. Ge, C. T. Lu and H. L. Wong, *J. Controlled Release*, 2014, **186**, 22–31.
20 M. Zhang, W. Z. Yu, X. T. Shen, Q. Xiang, J. Xu, J. J. Yang, P. P. Chen, Z. L. Fan, J. Xiao, Y. Z. Zhao and C. T. Lu, *Cardiovasc. Drugs Ther.*, 2016, **30**, 247–261.
21 L. Zhang, Z. Sun, P. Ren, M. You, J. Zhang, L. Fang, J. Wang, Y. Chen, F. Yan, H. Zheng and M. Xie, *Theranostics*, 2017, **7**, 51–66.
22 P. Yan, K. J. Chen, J. Wu, L. Sun, H. W. Sung, R. D. Weisel, J. Xie and R. K. Li, *Biomaterials*, 2014, **35**, 1063–1073.
23 W. Tzu-Yin, K. E. Wilson, S. Machtaler and J. K. Willmann, *Curr. Pharm. Biotechnol.*, 2013, **14**, 743–752.
24 P. Qin, T. Han, A. C. H. Yu and L. Xu, *J. Controlled Release*, 2018, **272**, 169–181.
25 R. Bekeredjian, S. Chen, P. A. Grayburn and R. V. Shohet, *Ultrasound Med. Biol.*, 2005, **31**, 687–691.
26 J. Suzuki, M. Ogawa, K. Takayama, Y. Taniyama, R. Morishita, Y. Hirata, R. Nagai and M. Isobe, *J. Am. Coll. Cardiol.*, 2010, **55**, 904–913.
27 W. S. Sheng, H. L. Xu, L. Zheng, Y. D. Zhuang, L. Z. Jiao, J. F. Zhou, D. L. ZhuGe, T. T. Chi, Y. Z. Zhao and L. Lan, *Artif. Cells, Nanomed., Biotechnol.*, 2018, 1–13, DOI: 10.1080/21691401.2018.1457538.
28 F. Yan, X. Li, Q. Jin, C. Jiang, Z. Zhang, T. Ling, B. Qiu and H. Zheng, *Ultrasound Med. Biol.*, 2011, **37**, 768–779.
29 J. Liu, Y. Chen, G. Wang, Q. Lv, Y. Yang, J. Wang, P. Zhang, J. Liu, Y. Xie, L. Zhang and M. Xie, *Biomaterials*, 2018, **162**, 200–207.
30 S. Stewart, G. L. Winters, M. C. Fishbein, H. D. Tazelaar, J. Kobashigawa, J. Abrams, C. B. Andersen, A. Angelini, G. J. Berry, M. M. Burke, A. J. Demetris, E. Hammond, S. Itescu, C. C. Marboe, B. McManus, E. F. Reed, N. L. Reinsmoen, E. R. Rodriguez, A. G. Rose, M. Rose, N. Suciu-Focia, A. Zeevi and M. E. Billingham, *J. Heart Lung Transplant.*, 2005, **24**, 1710–1720.
31 J. F. Delgado, V. Sanchez and C. S. de la Calzada, *Expert Opin. Pharmacother.*, 2006, **7**, 1139–1149.
32 C. R. Mayer, N. A. Geis, H. A. Katus and R. Bekeredjian, *Expert Opin. Drug Delivery*, 2008, **5**, 1121–1138.
33 T. Ishii, T. Asai, D. Oyama, Y. Agato, N. Yasuda, T. Fukuta, K. Shimizu, T. Minamino and N. Oku, *FASEB J.*, 2013, **27**, 1362–1370.
34 W. Xu, P. Ling and T. Zhang, *Int. J. Pharm.*, 2014, **460**, 173–180.
35 S. Khan, M. Shaharyar, M. Fazil, S. Baboota and J. Ali, *Eur. J. Pharm. Biopharm.*, 2016, **108**, 277–288.
36 J. J. Janicki, M. B. Chancellor, J. Kaufman, M. A. Gruber and D. D. Chancellor, *Toxins*, 2016, **8**, 81.

37 Y. Dai, R. Zhou, L. Liu, Y. Lu, J. Qi and W. Wu, *Int. J. Nanomed.*, 2013, **8**, 1921–1933.
38 R. Kojima, T. Yoshida, H. Tasaki, H. Umejima, M. Maeda, Y. Higashi, S. Watanabe and N. Oku, *Int. J. Pharm.*, 2015, **492**, 20–27.
39 R. K. Schlicher, H. Radhakrishna, T. P. Tolentino, R. P. Apkarian, V. Zarnitsyn and M. R. Prausnitz, *Ultrasound Med. Biol.*, 2006, **32**, 915–924.
40 S. Qin, C. F. Caskey and K. W. Ferrara, *Phys. Med. Biol.*, 2009, **54**, R27–R57.
41 Y. Guo, W. Chen, W. Wang, J. Shen, R. Guo, F. Gong, S. Lin, D. Cheng, G. Chen and X. Shuai, *ACS Nano*, 2012, **6**, 10646–10657.
42 R. de Waal Malefyt, H. Yssel and J. E. de Vries, *J. Immunol.*, 1993, **150**, 4754–4765.
43 H. O. Pae, G. S. Oh, B. M. Choi, S. C. Chae, Y. M. Kim, K. R. Chung and H. T. Chung, *J. Immunol.*, 2004, **172**, 4744–4751.
44 Y. L. Wang, Z. Q. Tang, W. Gao, Y. Jiang, X. H. Zhang and L. Peng, *Transplant Proc.*, 2003, **35**, 3024–3025.
45 N. Lipsman, Y. Meng, A. J. Bethune, Y. Huang, B. Lam, M. Masellis, N. Herrmann, C. Heyn, I. Aubert, A. Boutet, G. S. Smith, K. Hynynen and S. E. Black, *Nat. Commun.*, 2018, **9**, 2336.
46 S. Hernot, B. Cosyns, S. Droogmans, C. Garbar, P. Couck, C. Vanhove, V. Caveliers, G. Van Camp, A. Bossuyt and T. Lahoutte, *Ultrasound Med. Biol.*, 2010, **36**, 158–165.
47 H. Fujii, S. H. Li, J. Wu, Y. Miyagi, T. M. Yau, H. Rakowski, K. Egashira, J. Guo, R. D. Weisel and R. K. Li, *Eur. Heart J.*, 2011, **32**, 2075–2084.
48 E. Unger, T. Porter, J. Lindner and P. Grayburn, *Adv. Drug Delivery Rev.*, 2014, **72**, 110–126.
49 R. J. Plenter, M. R. Zamora and T. J. Grazia, *J. Invest. Surg*, 2013, **26**, 223–228.
50 J. Shan, Y. Huang, L. Feng, L. Luo, C. Li, N. Ke, C. Zhang and Y. Li, *J. Surg. Res.*, 2010, **164**, 155–161.